MOLECULAR AND CELLULAR BIOLOGY, Apr. 1995, p. 2037–2050 Vol. 15, No. 4
0270-7306/95/$04.00+0
Copyright © 1995, American Society for Microbiology

The *Saccharomyces SHP1* Gene, Which Encodes a Regulator of Phosphoprotein Phosphatase 1 with Differential Effects on Glycogen Metabolism, Meiotic Differentiation, and Mitotic Cell Cycle Progression

SHIRONG ZHANG, SUJATA GUHA, AND FREDRIC C. VOLKERT*

Department of Microbiology and Immunology and Morse Institute for Molecular Biology and Genetics, State University of New York Health Science Center at Brooklyn, Brooklyn, New York 11203-2098

Received 26 September 1994/Returned for modification 3 November 1994/Accepted 3 January 1995

The phosphoprotein phosphatase 1 (PP1) catalytic subunit encoded by the *Saccharomyces GLC7* gene is involved in control of glycogen metabolism, meiosis, translation, chromosome segregation, cell polarity, and G_2/M cell cycle progression. It is also lethal when overproduced. We have isolated strains which are resistant to Glc7p overproduction lethality as a result of mutations in the *SHP1* (suppressor of high-copy PP1) gene, which was previously encountered in a genomic sequencing project as an open reading frame whose interruption totally blocked sporulation and slightly slowed cell proliferation. These phenotypes also characterized our *shp1* mutations, as did deficient glycogen accumulation. Lysates from the *shp1* mutants were deficient in PP1 catalytic activity but exhibited no obvious abnormalities in the steady-state level or subcellular localization pattern of a catalytically active Glc7p-hemagglutinin fusion polypeptide. The lower level of PP1 activity in *shp1* cells permitted substitution of a galactose-induced *GAL10-GLC7* fusion for *GLC7*; depletion of Glc7p from these cells by growth in glucose medium resulted in G_2/M arrest as previously observed for a *glc7*^{cs} allele but with depletion arrest occurring most frequently at a later stage of mitosis. The higher requirement of glycogen accumulation and sporulation for PP1 activity would permit their regulation via Glc7p activity, independent of its requirement for mitosis.

During the last several years, studies employing fungal genetics have begun to make a major contribution to our understanding of the roles that serine/threonine phosphoprotein phosphatases (PPs) play in the control of vital processes in eukaryotic cells. The need for genetic analysis seems particularly acute for PP1 and PP2A, whose broad substrate and pathway specificities could hamper the resolution of regulatory questions by purely biochemical approaches (14, 44). The homolog of the mammalian PP1 catalytic subunit that is encoded by the *GLC7* gene of *Saccharomyces cerevisiae* is essential for viability (17). At its restrictive temperature, a *glc7*^{cs} mutant ceases growth at G_2/M (23), which is reminiscent of the M-phase growth arrest exhibited by PP1 conditional mutants of *Aspergillus nidulans* (15) and *Schizosaccharomyces pombe* (31, 32). Other, nonlethal mutations in *GLC7* implicate it in control of mitotic chromosome segregation (18), of glycogen metabolism (33), of meiosis and/or sporulation (11), of bud emergence (23), and of control of translation via dephosphorylation of eukaryotic initiation factor 2α (eIF-2α) (55). Wild-type *GLC7* is also lethal when overexpressed by fusion to a strong promoter (26) or by cloning on an inducible high-copy vector (see below). Lower levels of overexpression lead to decreased fidelity of chromosome segregation (18).

In its effect on these disparate processes, it is still unclear whether Glc7p is actively regulatory, i.e., variably affecting the target process in response to an upstream effector or signal, or whether it is merely acting as a counterpoise to one or more actively regulatory kinases. If Glc7p is to play an actively regulatory role, an issue to be resolved is whether and, if so, how it can control different pathways independently of each other. One possible solution, suggested by analogy with mammalian PP1s, is association of Glc7p with regulatory subunits which target it to particular substrates or subcellular compartments (14, 44). Gac1p, which is homologous to a mammalian PP1 glycogen-targeting subunit, may represent an example of this mode of regulation (19, 45). In this paper we report the identification of a direct or indirect positive effector of Glc7p activity, encoded by the *SHP1* (suppressor of high-copy PP1) gene, whose mutant phenotypes and biochemical effects imply that Glc7p may also be able to exert differential regulation of multiple pathways because they require different levels of its activity.

MATERIALS AND METHODS

Plasmids. pJH5 (54a) is a 9,818-bp plasmid consisting of pUC8 with the following yeast sequences inserted in its *Nde*I site after conversion of the *Nde*I cohesive termini to blunt ends with Klenow polymerase: the *LEU2 Hpa*I-*Sal*I fragment (3, 4), a *Hin*dIII fragment of the 2μm circle episome containing a *FRT* site for Flp1p-mediated recombination (bases 105 through 1017 of the standard map of the 2μm circle A isomer [22]; *Sal*I-*Hin*dIII junction created by blunt ligation of Klenow polymerase-filled cohesive termini), the *URA3 Hin*dIII fragment (36), and a *Hin*dIII-*Hpa*I fragment of the 2μm circle (bases 105 through 1684 of the B isomer [22]) containing another *FRT* site, the origin of replication, and the *STB* partition locus (10). Additionally, the *Sma*I-*Hpa*I fragment of YCp50 containing *CEN4* (39) is inserted in the *Sma*I site of the *URA3* 3′-flanking region, in the same orientation as in YCp50. Orientations of the components are shown in Fig. 1. pJH5*KAR1* was constructed by insertion of a 7.5-kb *Bam*HI fragment of pMR32 (gift of M. Rose), consisting of *KAR1* and flanking genomic sequences, into the *Bam*HI site in the pUC8 polylinker of pJH5. pJH5*HCL5* consists of pJH5 with an insertion of a 5.1-kb *Sau*3AI partial-digestion fragment of the *S. cerevisiae* S288C genome, including *GLC7*, in its *Bam*HI site. Its isolation from a pJH5-based genomic library is described in Results. pRC21 was constructed by insertion of the largest *Xmn*I-*Xba*I fragment of pFV17 (54), containing a fusion of the *GAL10* promoter to *FLP1*, into the *Xba*I site located

* Corresponding author. Mailing address: Department of Microbiology and Immunology, SUNY Health Science Center at Brooklyn, 450 Clarkson Ave., Box 44, Brooklyn, NY 11203-2098. Phone: (718) 270-2933. Fax: (718) 270-2656. Electronic mail address: volkert@medlib.hscbklyn.edu.

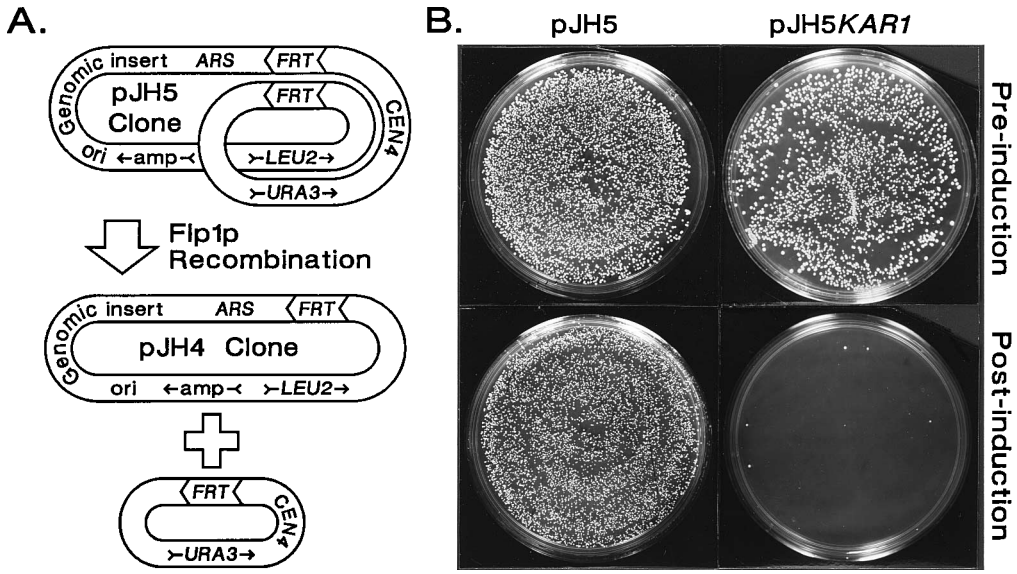

FIG. 1. Plasmid system for detection of the Hcl phenotype. (A) Schematic diagram showing rearrangement of a pJH5 library clone from its centromeric to its acentric (pJH4) form by Flp1p recombinase. Sequence elements are shown in the correct relationship and orientation but are not drawn to scale. (B) Negative and positive controls of the Hcl assay: strain RCY3-1C transformed with pJH5 and with pJH5*KAR1*, respectively. A total of 10^4 cells were spread on −Leu plates before and after galactose induction of *FLP1* transcription. In RCY3-1C(pJH5*KAR1*) and other RCY3-1C(pJH5*HCL*) strains, more than 90% of residual Leu^+ CFU after galactose induction result from failure of the plasmid to recombine or from reversal of the recombination and more than 90% of the remainder result from chromosomal integration of the plasmid or gene conversion of the chromosomal *leu2* allele (21a).

3′ to *HIS3* in pMM62 (29; gift of J. Broach), using *Xba*I linkers. pSRZ15 was constructed by subcloning the *Xho*I fragment of the *HCL5* genomic insert containing *GLC7* into the *Sal*I site of pUC8 and then replacing the part of the *GLC7* coding region extending from *Sal*I to *Bgl*II with the *LEU2 Xho*I-*Sal*I fragment derived from plasmid TLC1 (9; gift of J. Broach); the *Sal*I and *Bgl*II ends were converted to *Xho*I by Klenow filling and attachment of linkers. pSRZ17 was constructed by PCR-mediated amplification of the *GLC7* coding region and 3′-flanking sequences from pJH5*HCL5* with primers that added a 5′ *Xho*I site and a 3′ *Hin*dIII site, cleavage of the product with those two enzymes, and substitution of the resulting *Xho*I-*Hin*dIII fragment for the *Sal*I-*Hin*dIII fragment containing the 5′ end of the *FLP1* gene in the *GAL10-FLP1* fusion plasmid pFV17 (54). The primers for the 5′ end of the coding region and for the 3′-flanking region had the sequences 5′-CCCCCCTCGAG*ATG*GACTCACA ACCAGTTGACG-3′ and 5′-CCCCCAAGCTTCCAAAGGAAGACGTGACC ATT-3′, respectively (32), where the restriction sites are underlined and the initiation codon is in italic type. pSRZ24 was constructed by conversion of the unique *Stu*I site of pSRZ17 to a *Xho*I site with a linker followed by the insertion, into that site, of the smaller *Xho*I fragment of pFV8, which contains a portable *LYS2* interruption cassette (54). pSRZ27 is a derivative of YIp5 in which the *Sal*I-*Bam*HI fragment in the *tet*^{r} gene has been replaced with the fragment of the *shp1*-complementing YCp50 library clone 5 (see Results) that extends from the YCp50 *Sal*I site, 276 bp to the left of the insert shown in Fig. 9, to the *Bam*HI site within *SHP1* in the insert. pJL5 was constructed by insertion of the *Xho*I fragment of the *HCL5* genomic insert containing *GLC7* into the unique *Sal*I site of YCp50. CB597 (49; gift of K. Arndt) is a YCp50 clone of *GLC7* with an insertion of a sequence encoding an influenza virus hemagglutinin (HA) epitope (YPYDVPYDYAT) recognized by monoclonal antibody 12CA5 after the initiator methionine. pd13, pd46, and p1833 (all gifts of J. Cannon) are YEp24 (6) clones of genomic *GLC1* and *GLC4* and a YCp50 clone of genomic *GLC8*, respectively. B1311 (gift of M. Rose) is a YCp50 clone of *MAT*α. YCp50 (39) was a gift of M. Rose, and YIp5 (47) and pUC8 (53) were gifts of J. Broach.

Yeast strains. Table 1 shows the genotypes of *S. cerevisiae* strains used in this study. Other than S288C, all were ultimately derived from the closely related [cir^0] strains S150-2B[cir^0], 4-18D, and MM1 (8, 29; gifts of J. Broach) via standard meiotic crosses and specific genome alterations described in this paper and reference 54. The *HIS3*::*GAL10-FLP1* allele was constructed by one-step gene replacement (41) of *his3*Δ with the smaller *Bam*HI fragment of pRC21. The *lys2*::(*LEU2 GAL10-GLC7*) allele was constructed by one-step gene replacement of *LYS2* with *Nco*I-cleaved pSRZ24, using the portable disruption cassette technique described in reference 54. *glc7*::*LEU2*/*GLC7* heterozygotes were constructed by one-step gene replacement of one copy of *GLC7* in homozygous diploid strains with *glc7*::*LEU2*, using *Pst*I-*Hin*dIII-cleaved pSRZ15. Viable haploid strains bearing *glc7*::*LEU2* were constructed by tetrad dissection of *glc7*::*LEU2*/*GLC7* heterozygotes carrying *GLC7* or *GLC7*::HA genes on *CEN* plasmids (i.e., pJH5*HCL5*, pJL5, and CB597). Plasmid-free derivatives of haploid *shp1 glc7*::*LEU2* strains that contained *GAL10-GLC7* fusions were isolated from YPGal cultures (see below). Lethality of the *glc7*::*LEU2* alleles in haploid segregants was verified by the inability of the strains to lose their *GLC7* or *GLC7*::HA plasmids during growth in nonselective media or, for the plasmid-free *shp1 GAL10-GLC7* derivatives, by galactose-dependent growth. The correct structure of gene replacements was verified by Southern blotting (data not shown).

High-copy lethality assay. Late-exponential-phase cultures of strain RCY3-1C, transformed with pJH5 carrying a putative high-copy lethal (*HCL*) insertion and grown in −Leu −Ura raffinose medium (see below), were diluted into SCGal medium to induce *FLP1* expression for 45 min to 1 h. After brief sonication to disaggregate clumped cells, pre- and postinduction cells were spread on −Leu glucose plates (see below) at 10^4 cells per plate. Colonies were observed after 2 to 3 days. Cells originally transformed with pJH5 lacking an insert, or carrying a non-*HCL* insert, founded normal-sized colonies under these conditions at high efficiency (>50%), but those whose pJH5 inserts were *HCL* founded such colonies 2 orders of magnitude less frequently (Fig. 1); the difference was made up by pinpoint-to-very-small colonies whose size was characteristic for each particular *HCL* gene (too small to be seen in Fig. 1 and 2; visible at higher magnification in Fig. 3). For library and suppression screening, the assay was performed essentially as described in the preceding sentences, using small-scale cultures grown on a nutating platform in 96-well dishes. Then, cells were plated after induction by carefully removing a loopful of culture supernatant without disturbing sedimented cells and streaking a one-sixth sector of a −Leu plate (Fig. 3).

Immunofluorescence staining and photomicrography. Formaldehyde fixation and immunofluorescence staining of yeast cells were performed as described in reference 34. We stained microtubules with YOL1/34 rat monoclonal anti-yeast α-tubulin primary antibody (Sera Lab) diluted 1:100 and rhodamine-conjugated goat anti-rat immunoglobulin G secondary antibody (Sigma) diluted 1:400. We stained the *GLC7*::HA fusion protein with 12CA5 mouse monoclonal anti-HA primary antibody (BABCO) diluted 1:128 and fluorescein isothiocyanate-conjugated sheep anti-mouse immunoglobulin G secondary antibody (Sigma) diluted 1:200. For DNA staining, 4′,6-diamidinophenylindole (DAPI) was added to the mounting solution at 1 μg/ml. Epifluorescence and Nomarski differential interference contrast photomicrography were performed with a Nikon Labophoto-II photomicroscope with a 100× objective and Kodak Tri-X Pan or Ektachrome 400 film.

DEAE-cellulose chromatography of PPs. Steady-state experiments employed 200-ml early-stationary-phase (180 Klett units) yeast cultures grown in yeast extract-peptone-dextrose (YPD). For *GLC7* overexpression experiments, cells were transferred from those cultures to 200 ml of YPRaf medium, incubated for 8 h, transferred to 200 ml of YPGal medium, and incubated for 2 h. Inocula for the YPRaf cultures were adjusted so that the final density of the YPGal cultures was approximately the same as that of the YPD cultures. Cells were harvested by centrifugation at 4,000 × *g* in a GSA rotor for 5 min, washed with 100 ml of ice-cold water, and repelletted, and the pellets were frozen at −70°C. Frozen cell

TABLE 1. Yeast strains used in this study[a]

Strain	Genotype[b]
FVY2-6B	*MAT*α *leu2-3,112 ura3-52 his3*Δ [cir^0]
FVY9147	*MAT***a** *leu2-3,112 ura3-52 HIS3*::*GAL10-FLP1 shp1-2 steX* [cir^0]
FVY91123	*MAT***a**/*MAT*α *leu2-3,112*/*leu2-3,112 ura3-52*/*ura3-52 HIS3*::*GAL10-FLP1*/+ *his5-2*/+ *ade2*/+ [cir^0]
FVY91123-4D	*MAT*α *leu2-3,112 ura3-52 HIS3*::*GAL10-FLP1 ade2* [cir^0]
FVY91131	*MAT***a** *leu2-3,112 ura3-52 HIS3*::*GAL10-FLP1 shp1-1* [cir^0]
FVY91175	*MAT***a**/*MAT*α *leu2-3,112*/*leu2-3,112 ura3-52*/*ura3-52 ade2*/+ *HIS3*::*GAL10-FLP1*/*HIS3*::*GAL10-FLP1 shp1-1*/+ [cir^0]
FVY91175-1C	*MAT*α *leu2-3,112 ura3-52 HIS3*::*GAL10-FLP1 shp1-1* [cir^0]
FVY91193	*MAT***a**/*MAT*α *leu2-3,112*/*leu2-3,112 ura3-52*/*ura3-52 HIS3*::*GAL10-FLP1*/*HIS3*::*GAL10-FLP1 ade2*/+ *shp1-2*/+ *steX*/+ [cir^0]
FVY91193-1C	*MAT*α *leu2-3,112 ura3-52 HIS3*::*GAL10-FLP1 shp1-2* [cir^0]
FVY92006	*MAT***a**/*MAT*α *leu2-3,112*/*leu2-3,112 ura3-52*/*ura3-52 HIS3*::*GAL10-FLP1*/*HIS3*::*GAL10-FLP1 ade2*/+ *shp1-1*/*shp1-2* [cir^0]
FVY92007	*MAT***a**/*MAT*α *leu2-3,112*/*leu2-3,112 ura3-52*/*ura3-52 HIS3*::*GAL10-FLP1*/*HIS3*::*GAL10-FLP1 ade2*/+ *shp1-1*/*shp1-1* [cir^0]
FVY92008	*MAT***a**/*MAT*α *leu2-3,112*/*leu2-3,112 ura3-52*/*ura3-52 HIS3*::*GAL10-FLP1*/*HIS3*::*GAL10-FLP1 ade2*/+ *shp1-2*/*shp1-2* [cir^0]
FVY92186	*MAT***a** *leu2-3,112 ura3-52 HIS3*::*GAL10-FLP1 lys2*::(*LEU2 GAL10-GLC7*) [cir^0]
FVY92189	*MAT*α *leu2-3,112 ura3-52 HIS3*::*GAL10-FLP1 lys2*::(*LEU2 GAL10-GLC7*) *shp1-1* [cir^0]
FVY92192	*MAT*α *leu2-3,112 ura3-52 his3*Δ *lys2*::(*LEU2 GAL10-GLC7*) [cir^0]
FVY92206	*MAT***a**/*MAT*α *leu2-3,112*/*leu2-3,112 ura3-52*/*ura3-52 ade2*/+ *HIS3*::*GAL10-FLP1*/*HIS3*::*GAL10-FLP1 lys2*::(*LEU2 GAL10-GLC7*)/*lys2*::(*LEU2 GAL10-GLC7*) [cir^0]
FVY92215-2D	*MAT***a** *leu2-3,112 ura3-52 HIS3*::*GAL10-FLP1 lys2*::(*LEU2 GAL10-GLC7*) *shp1-1* [cir^0]
FVY92215-9A	*MAT*α *leu2-3,112 ura3-52 his3*Δ *lys2*::(*LEU2 GAL10-GLC7*) *shp1-1* [cir^0]
FVY93012	*MAT***a**/*MAT*α *leu2-3,112*/*leu2-3,112 ura3-52*/*ura3-52 HIS3*::*GAL10-FLP1*/*his3*Δ *ade2*/+ *lys2*::(*LEU2 GAL10-GLC7*)/+ *glc7*::*LEU2*/+ *shp1-1*/+ [cir^0]
FVY93014	*MAT*α *leu2-3,112 ura3-52 his3*Δ *lys2*::(*LEU2 GAL10-GLC7*) *glc7*::*LEU2 shp1-1* [cir^0]
FVY93043	*MAT*α *leu2-3,112 ura3-52 his3*Δ *glc7*::*LEU2 lys2*::(*LEU2 GAL10-GLC7*) *shp1-1* [*URA3 GLC7*::HA] [cir^0]
FVY93044	*MAT***a** *leu2-3,112 ura3-52 HIS3*::*GAL10-FLP1 glc7*::*LEU2* [*URA3 GLC7*::HA] [cir^0]
FVY93140	*MAT*α *leu2-3,112 ura3-52 HIS3*::*GAL10-FLP1 lys2*::(*LEU2 GAL10-GLC7*) *shp1-2* [cir^0]
FVY93142	*MAT***a**/*MAT*α *leu2-3,112*/*leu2-3,112 ura3-52*/*ura3-52 his3*Δ/*HIS3*::*GAL10-FLP1 lys2*::(*LEU2 GAL10-GLC7*)/*lys2*::(*LEU2 GAL10-GLC7*) *shp1-1*/+ [cir^0]
FVY93146	*MAT***a**/*MAT*α *leu2-3,112*/*leu2-3,112 ura3-52*/*ura3-52 his3*Δ/*HIS3*::*GAL10-FLP1 lys2*::(*LEU2 GAL10-GLC7*)/*lys2*::(*LEU2 GAL10-GLC7*) *glc7*::*LEU2*/+ *shp1-1*/+ [*URA3 GLC7*::HA] [cir^0]
FVY93149	*MAT*α *leu2-3,112 ura3-52 HIS3*::*GAL10-FLP1 glc7*::*LEU2 shp1-1* [*URA3 GLC7*::HA] [cir^0]
RCY3-1C	*MAT***a** *leu2-3,112 ura3-52 HIS3*::*GAL10-FLP1* [cir^0]
S288C	*MAT*α *mal gal2*

[a] Construction of FVY2-6B is described in reference 54. S288C is described in reference 40. The remaining strains were constructed in the course of this work.
[b] *steX* is an uncharacterized strong sterile allele recovered in the same isolate (i.e., FVY9147) as *shp1-2* after EMS treatment of RCY3-1C(pJH5*HCL5*). The *steX* heterozygote FVY91193 was constructed by polyethylene glycol-mediated spheroplast fusion of FVY9147 and FVY91123-4D, and all other *shp1-2* strains are derived from it. The sterile phenotype segregated independently of *GLC7* overexpression lethality suppression and of mating type in the meiotic progeny of FVY91193 (data not shown), and none of the derivative *shp1-2* strains listed above is sterile.

pellets were suspended in 1 ml of buffer A [50 mM Tris-HCl (pH 7.4), 0.2 mM EDTA, 0.2 mM ethylene glycol-bis(β-aminoethyl ether)-*N*,*N*,*N*′,*N*′-tetraacetic acid (EGTA), 1 mM phenylmethylsulfonyl fluoride] and lysed by addition of 1 ml of acid-washed glass beads and four cycles of vortex mixing at 4°C for 2 min alternating with chilling on ice for 2 min. Extracts were clarified by full-speed centrifugation in a microcentrifuge for 15 min at 4°C, diluted to 4 ml with ice-cold buffer A, and applied to a 3-ml DEAE-cellulose column which had been preequilibrated with buffer A. Within each experiment (i.e., fractionation of the two extracts in Fig. 7A and of the four in Fig. 7B), the same amount of protein was used for each column run. The column was washed with 5 ml of buffer A and eluted with 20 ml of a linear salt gradient (0 to 0.5 M NaCl) in buffer A, and 0.5-ml (see Fig. 7A) or 1-ml (see Fig. 7B) fractions were collected.

PP assay. We measured the PP activity in DEAE-cellulose chromatography fractions as release of soluble ^{32}P from labeled glycogen phosphorylase *a*, using the Gibco BRL Protein Phosphatase Assay System. We labeled and purified the substrate by using kit protocols and materials and reacted 20 μl of purified substrate with 20 μl of full-strength or diluted (in assay buffer) column fraction and 20 μl of protein phosphatase assay buffer (20 mM imidazole-HCl [pH 7.63], 0.1% β-mercaptoethanol, 1 mg of bovine serum albumin per ml, 0.1 mM EDTA, 0 or 2 nM okadaic acid). Reactions were stopped and substrate precipitated after a 10-min incubation at 30°C by addition of 180 μl of ice-cold 20% trichloroacetic acid. After centrifugation for 3 min at full speed in a microcentrifuge, the acid-soluble ^{32}P in 200 μl of supernatant was measured by scintillation counting. A PP unit was defined as release of 10^{-9} nmol of ^{32}P min^{-1} by 1 μl of column fraction.

Cell fractionation and Western immunoblotting. Nuclear and cytoplasmic fractions of strains FVY93043 and FVY93044 were prepared by percoll gradient fractionation (2). In these experiments, "total-cell lysate" refers to the cleared prenuclear supernatant, "cytoplasm" refers to the postnuclear supernatant, and "nuclei" refers to the Percoll gradient fraction. Fractions were analyzed by sodium dodecyl sulfate-polyacrylamide gel electrophoresis through a 12.5% gel. Per-lane loadings were 10 mg of protein from the total-cell lysates and cytoplasmic fractions and 5 mg of protein from the nuclei. The resolved protein bands were transferred to nitrocellulose membrane and detected by the ECL Western Blotting Analysis System (Amersham Life Science).

Miscellaneous methods. Routine yeast media were made according to the formulas in reference 40, and strains were grown at 30°C in or on YPD unless other conditions are specified. Selection for hybrid or transformed strains was done with synthetic complete (SC) medium lacking one or two defined nutrients, notated as -Leu, -Ura -His, etc. Substitution of 2% galactose or raffinose for glucose is notated as YPGal, -Ura raffinose, etc. Medium for determination of nitrogen starvation sensitivity was prepared as described in reference 52. Ethyl methanesulfonate (EMS) mutagenesis was performed as described in reference 40, with EMS treatments of 15 and 30 min. Yeast transformation was performed by the lithium acetate procedure (24). Polyethylene glycol-mediated spheroplast fusion was performed by subjecting a mixture of the strains to be fused to the manipulations described for polyethylene glycol-mediated transformation (40), omitting the transforming DNA, and omitting from the plating medium auxotrophic nutrients appropriate to select fusion strains. Glycogen accumulation in yeast colonies was estimated semiquantitatively by carefully flooding plates with 5 ml of 0.2% I_2–0.4% KI solution and photographing the result after 2 min (52). Recombinant DNA manipulations were performed as described in reference 42 with enzymes obtained from New England Biolabs except where otherwise noted. The library of partially *Sau*3AI-digested *S. cerevisiae* S288C genomic DNA was cloned in *Bam*HI-cleaved, dephosphorylated pJH5 as described in reference 37. Oligonucleotides were obtained from the SUNY-HSCB Morse Institute DNA Core Facility. Southern blotting (12) was performed at normal stringency with ^{32}P-labeled probes prepared by the Bethesda Research Labora-

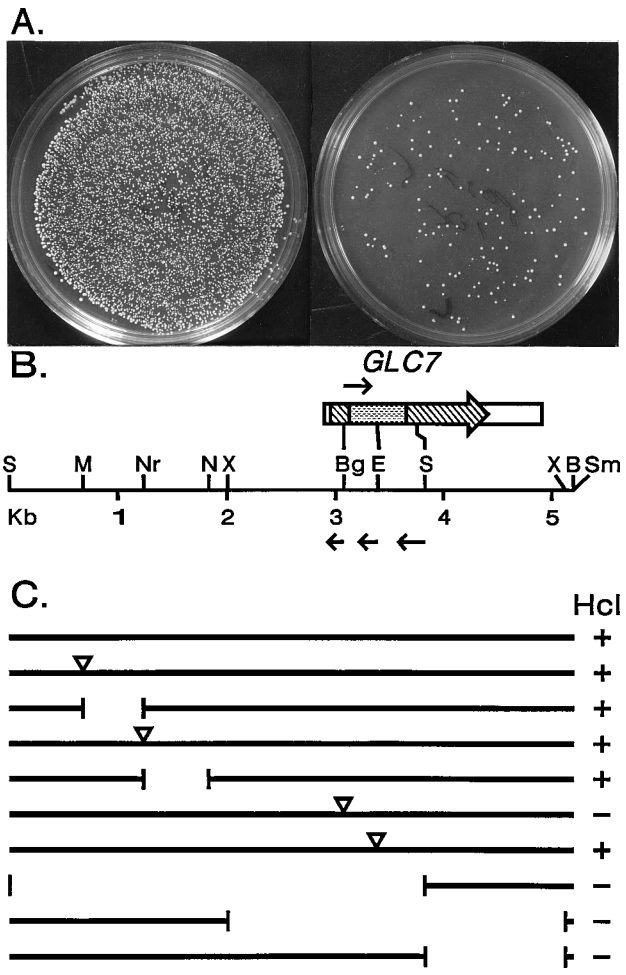

FIG. 2. Hcl phenotype of *GLC7*. (A) RCY3-1C(pJH5*HCL5*) cells (10^4 cells) were plated on −Leu medium before (left) and after (right) galactose induction of *FLP1* transcription. (B) Our deduced restriction map of the *HCL5* genomic insertion (lower line) is shown aligned with the map predicted by the sequence of *GLC7* (17, 32; upper line). The lower map is displayed with the polylinker *Sal*I site of the vector on the left and its *Sma*I site on the right. Both maps are drawn to the same scale and are arbitrarily aligned at the unique *Bgl*II site. The stippled region of the upper map denotes the *GLC7* intron, and the remainder of the coding region is hatched. The small arrows above the upper line and beneath the lower line represent the sequences of the *HCL5* genomic insert that we determined, which were more than 98% identical to the corresponding segments of the published *GLC7* sequences. (C) Constructed mutations of *HCL5* and their effects on its Hcl phenotype. Deletions are shown as gaps. Triangles denote frameshifting *Not*I linker insertions. Insertion points and deletion end points are aligned with the *HCL5* deduced restriction map (lower line in panel B). Abbreviations: B, *Bam*HI; Bg, *Bgl*II; M, *Mlu*I; N, *Nhe*I; Nr, *Nru*I; S, *Sal*I; Sm, *Sma*I; X, *Xho*I.

tories nick translation kit. PCR was performed in a Perkin Elmer-Cetus thermal cycler with the GeneAmp kit (Perkin Elmer-Cetus). DNA sequencing was performed with the Sequenase kit (U.S. Biochemical). Protein concentrations were determined with the Bio-Rad protein assay system.

RESULTS

***shp1* mutations suppress high-copy lethality of *GLC7*.** We recovered *GLC7* during a screen of the yeast genome for *HCL* sequences. The design of the screen and its results will be reported in more detail elsewhere; briefly, it was performed with a yeast replicating vector of novel design, pJH5, whose copy number is initially centromere limited (13, 20, 46) but can be induced to increase 10- to 20-fold (21a) as a result of in vivo

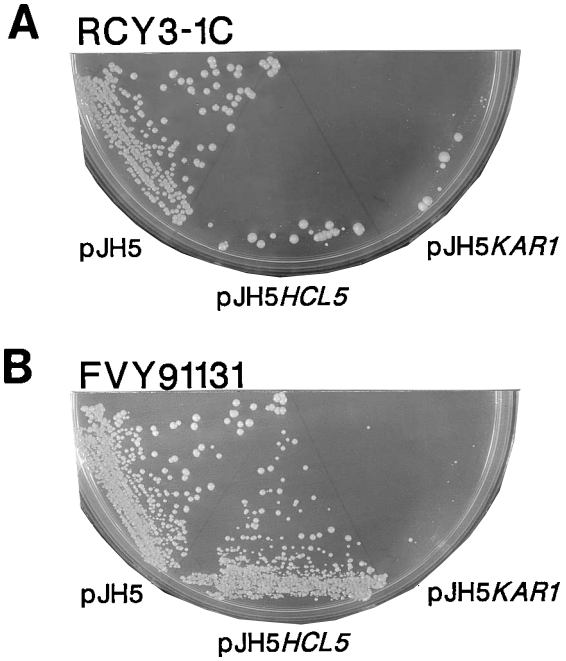

FIG. 3. Suppression of *GLC7* high-copy lethality by the *shp1-1* mutation. The screening assay for the Hcl phenotype was performed as described in Materials and Methods. (A) From left to right, the parental strain RCY3-1C transformed with pJH5, pJH5*HCL5*, and pJH5*KAR1*. (B) From left to right, FVY91131, the plasmid-free derivative of a primary suppressive isolate obtained from EMS mutagenesis of RCY3-1C(pJH5*HCL5*), transformed with the same three plasmids. Colony formation of all transformants before induction of Flp1p recombination was indistinguishable from the postinduction results obtained with the pJH5-bearing strains (data not shown).

excision of its centromere by controlled site-specific recombination mediated by Flp1p recombinase (7, 54) (Fig. 1). We cloned a library of *Sau*3AI partial digestion fragments of *S. cerevisiae* S288C genomic DNA in pJH5, amplified it in *Escherichia coli*, used it to transform yeast strain RCY3-1C, and then induced centromere excision from the library clones by galactose induction of a *GAL10-FLP1* promoter fusion. Individual examination of 8,074 transformants revealed 883 primary isolates whose colonies initially grew normally under selection for the *LEU2* marker of the vector but showed different degrees of growth retardation after centromere excision. Of 47 confirmed *HCL* isolates whose postexcision growth retardation was the most severe, 21 contained identical 5.1-kb insertions. Deletion and linker insertion mutagenesis of one of these inserts, *HCL5*, showed that its Hcl phenotype depended on the presence of an intact *GLC7* gene (Fig. 2).

As an approach to identifying biologically significant regulators or substrates of PP1 in *S. cerevisiae*, we sought to induce extragenic mutations which would suppress the high-copy lethality of *GLC7*. We treated RCY3-1C(pJH5*HCL5*) cells with EMS to effect 60 and 10% viability levels and tested 1,248 plasmid-bearing survivors individually for the Hcl phenotype. Of these, 11 showed different degrees of loss of the phenotype (data not shown). We used genetic tests to assess the reproducibility, specificity, and meiotic segregation pattern of the suppression of the Hcl phenotype of *GLC7* exhibited by these isolates and to determine their ploidy (Table 2). This analysis revealed that most of the isolates (7 or 8 of 11) were diploid derivatives of the haploid host strain, which had evidently arisen through endomitosis or self-mating and which could partially suppress the Hcl phenotypes of *GLC7* and other un-

TABLE 2. Genetic analysis of primary suppressive isolates of RCY3-1C(pJH5*HCL5*)[a]

Class	No. of isolates	Hcl suppression[b] of:		Tetrad analysis of B1311 transformant[c]					Tetrad analysis of FVY91123-4D hybrid[d]					Conclusion
		GLC7	*KAR1*	% Sporulation	% Viability	Segregation			% Sporulation	% Viability	Segregation			
						Mat	Leu	Shp[e]			Mat	Ade	Shp	
A	7	Weak	Weak	≈5	>90	$4^a:0^\alpha$	$0^+:4^-$	$4^+:0^{-f}$	≈5	≈10	ND[g]	ND	ND	WT[h] diploid[i]
B	1	Weak	Weak	0 (<0.01)					0 (<0.01)					*SPO*$^-$ or *mat*$^-$ diploid?
C	1	None	None	ND					ND					WT haploid
D	2	Strong	None	0 (<0.01)					≈5	>90	$2^a:2^\alpha$	$2^+:2^-$	$2^+:2^-$	*shp*$^-$ haploid

[a] Relevant genotype, *MAT***a** *leu2 ura3 ADE2 HIS3*::*GAL10-FLP1 SHP*$^+$ [*LEU2 URA3 GLC7*].
[b] Plasmid-free derivatives of primary isolates were identified by replica plating and were retransformed with pJH5*HCL5* (=*GLC7*) and with a pJH5 clone of an unrelated strong *HCL* gene, *KAR1* (21a, 38). The Hcl phenotypes of six transformants of each isolate with each plasmid were assessed, yielding fully congruent results. Figure 3B shows examples of strong suppression (pJH5*HCL5*) and nonsuppression (pJH5*KAR1*). Weak suppression results in the appearance of very small colonies whose cells can be serially propagated on −Leu plates, in place of the inviable microcolonies observed in the absence of suppression (data not shown).
[c] Plasmid-free derivatives of primary isolates were transformed with B1311 (=YCp50::*MAT*α), and sporulation was induced on plates. Sporulation of 1 to 10% is normal in this strain background (53a).
[d] Primary isolates were hybridized with FVY91123-4D (relevant genotype, *MAT*α *ade2*), and sporulation was induced on plates. Hybridization was accomplished by mating except for one sterile class D isolate, which required polyethylene glycol-mediated spheroplast fusion (see Table 1, footnote *b*).
[e] Shp, suppression of high-copy lethality of *GLC7*-PP1. +, nonsuppressive (*GLC7* remains Hcl); −, suppressive.
[f] Progeny of tetrads derived from two of seven primary isolates were retransformed with pJH5*HCL5* and were scored for Shp$^{+/-}$.
[g] ND, not done.
[h] WT, wild type.
[i] We have also observed weak suppression of the Hcl phenotypes of *GLC7* and *KAR1* in deliberately constructed *MAT***a**/*MAT***a** and *MAT***a**/*MAT*α diploid strains that have not been mutagenized (57) and have recovered spontaneous diploid strains as weak suppressors of other unrelated *HCL* genes (26a).

related *HCL* genes by virtue of their ploidy. However, 2 of 11 primary isolates (Table 2, class D), designated FVY91131 and FVY9147, were haploid descendants of RCY3-1C which had acquired chromosomal mutations that specifically and strongly suppressed the Hcl phenotype of *GLC7*. Since the complementation data presented below indicate that they are allelic, we have designated the suppressive mutations in FVY91131 and FVY9147 as *shp1-1* and *shp1-2* (for suppressor of high-copy PP1), respectively.

***shp1* mutations suppress lethality of an induced *GAL10-GLC7* fusion.** We integrated a fusion of the *GAL10* promoter to the *GLC7* coding region at the *LYS2* loci of *shp1-1*, *shp1-2*, and control strains. As expected (26), induced expression of the fusion was severely toxic in the wild-type cells (Fig. 4). In contrast with the previous report (26), however, we observed striking morphological consequences of *GLC7* overexpression (Fig. 5). While the cells did not exhibit cell cycle stage-specific arrest of growth, a high percentage of them exhibited one of two pathological terminal morphologies: unbudded and with a short spindle but abnormally large and round (68%); or with bizarre, abnormally elongated buds (15%). During the course of arrest, the latter group exhibited an elongated nucleus, extending into both cells, and an elongated spindle; however, both nuclear lobes and both spindle poles were frequently seen in the same cell body (e.g., one cell in Fig. 5C and D). At late times after galactose induction, no organized nucleus or spindle could be visualized in most cells by DNA or tubulin staining (data not shown).

As shown in Fig. 4 and 5, the *shp1-1* mutation suppressed overexpression toxicity of *GAL10-GLC7* at the level of growth, viability, and morphology, which implies that its primary suppression of the Hcl phenotype of *GLC7* was not a result of an effect on plasmid population dynamics but, rather, of a decrease in concentration or activity of Glc7p, or in the response of the cells to Glc7p activity. The suppression of *GAL10*-driven overexpression lethality by this mutation additionally argues against the effects of the mutation being related to control of transcription from the *GLC7* promoter. In contrast, the ploidy effects on susceptibility to *GLC7* high-copy lethality, described above, did not carry over to overexpression lethality of the fusion gene: wild-type *MAT***a**/*MAT*α diploid strains homozygous or heterozygous for the *lys2*::*GAL10-GLC7* allele remained normally susceptible (data not shown).

The *shp1* mutations confer recessive deficiency in glycogen accumulation and sporulation and define a single complementation group unlinked to *GLC7*. The prototypic mutant allele of *GLC7*, *glc7-1*, confers deficiency in glycogen accumulation and in sporulation without ablating the essential function of Glc7p (11, 33). We assessed these phenotypes in *shp1-1* and *shp1-2* haploid strains, in homozygous and simply heterozygous mutant diploid strains, and in *shp1-1*/*shp1-2* heterozygotes. The results of these studies, shown in Fig. 6 and Table 3, indicated that the *shp1-1* and *shp1-2* mutations also conferred recessive deficiency in glycogen accumulation, as measured by iodine staining, and in meiotic differentiation, as measured by spore formation, and that, further, they failed to complement each other's deficiencies in these phenotypes. Additionally, in strain FVY92189 (*GLC7 GAL10-GLC7 shp1-1*), induction of the *GAL10-GLC7* fusion suppressed the Glc$^-$ phenotype of the *shp1* mutation, in contrast to strain FVY91175-1C (*GLC7 shp1-1*), which remained Glc$^-$ on YPGal plates (data not shown). Together with their repeated coisolation in primary mutant strains, cosegregation of the suppressive (Shp$^-$), Glc$^-$, and Spo$^-$ phenotypes in meiotic tetrads from a *shp1-1* heterozygote indicated that they were all manifestations of mutations in one gene (Table 4).

Deficiency in accumulation of storage carbohydrates and deficiency in the ability to commit to meiotic differentiation are also hallmarks of mutations in a variety of genes that result in unregulated or excessive activity of cyclic AMP (cAMP)-dependent protein kinase (11, 21, 27, 50–52). Typically, however, such mutations produce a pleiotropic deficiency in G_0-phase physiologic adaptations, including not only those associated with *glc7-1* but also those that enable the cell to withstand stressful conditions such as heat shock and nutrient limitation. We tested wild-type and *shp1-1* and *shp1-2* mutant strains for their sensitivity to heat shock and to nitrogen deprivation by replica plating patches of them grown on YPD at 30°C to

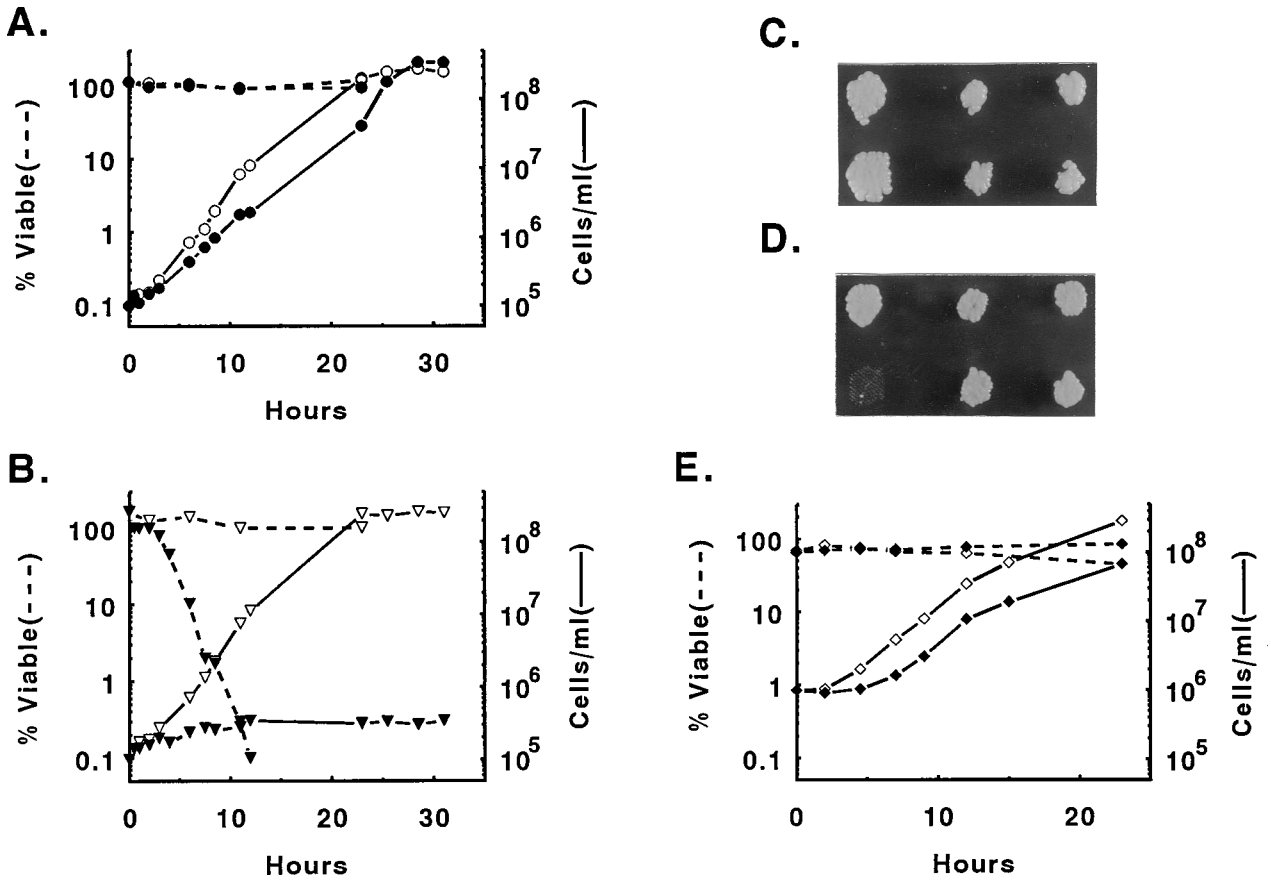

FIG. 4. Suppression of *GAL10-GLC7* overexpression lethality by the *shp1* mutations. (A) Growth and viability of the *GLC7 SHP1* strain FVY2-6B after transfer from YPRaf medium to YPD (open symbols) or YPGal (solid symbols). (B) Growth and viability of the *GAL10-GLC7 SHP1* strain FVY92192 under the same conditions as in panel A. (C and D) Patches of mutant and control strains were replica plated from YPD plates to YPD (C) and YPGal (D) plates. Top row, *GLC7* strains; left to right: RCY3-1C (*SHP1*), FVY91175-1C (*shp1-1*), and FVY91193-1C (*shp1-2*). Bottom row, *GAL10-GLC7* strains; left to right: FVY92186 (*SHP1*), FVY92189 (*shp1-1*), and FVY93140 (*shp1-2*). (E) Growth and viability of the *GAL10-GLC7 shp1-1* strain FVY92215-9A under the same conditions as in panel A.

low-nitrogen medium and to YPD plates which were incubated at 57°C for 15 min and 50°C for 1 h (50, 51). The results failed to demonstrate any difference between the wild type and mutant strains (data not shown), indicating that the defects in *shp1* mutant strains are unlikely to affect control of cAMP-dependent protein kinase activity. Also favoring this interpretation are the observations that *shp1* strains do not exhibit a rapid loss of viability after nutrient exhaustion in liquid cultures (see, e.g., Fig. 4) and that they remain highly viable for more than 1 month on YPD plates stored at 4°C (56).

Since the *shp1* mutations were recessive but suppressed the dominant overexpression lethal phenotype of the wild-type *GLC7*, they were very unlikely to be alleles of *GLC7*. Nevertheless, the similarity of their secondary phenotypes to those of *glc7-1* prompted us to formally rule out this possibility. When we dissected meiotic tetrads of the *shp1-1*/*SHP1*$^+$ *glc7*::*LEU2*/*GLC7*$^+$ diploid strain FVY93146, which was also homozygous for a *GAL10-GLC7* insertion at the *LYS2* locus, on YPD plates, viability segregated 2:2 as expected (17; data not shown). Cells derived from 9 of 18 viable (and, therefore, *GLC7*$^+$) spores suppressed lethality of the galactose-induced fusion, and those from the other 9 did not, demonstrating that *shp1-1* is not an allele of *GLC7*. Also, in another cross, a *his3* allele and *shp1-1* segregated at random, implying that *shp1-1* is not an allele of *GAC1*, which is linked to *HIS3* (30; Table 4).

Strains bearing *shp1* mutations exhibit an increased generation time. During genetic analysis of the *shp1* mutations we observed cosegregation of small colony size with the suppressive phenotype (Fig. 6; Table 4). This defect characterized colonies founded by vegetative cells, as well as those grown from spores, was seen (on YPD plates) both in strains that did and in strains that did not harbor *GAL10-GLC7* fusions and was not noticeably exacerbated or ameliorated by growth at 23 or 37°C (data not shown). This secondary phenotype of *shp1* mutations was also observed in liquid culture. In the experiments shown in Fig. 4, FVY92215-9A (*shp1-1 GLC7 GAL10-GLC7* [Fig. 4E]) had a generation time of 138 min during exponential growth in YPD liquid, compared with 97 min for FVY92192 (*SHP1 GLC7 GAL10-GLC7* [Fig. 4B]) and 90 min for FVY2-6B (*SHP1 GLC7* [Fig. 4A]). In another experiment in which growth in liquid YPD of FVY92215-9A and FVY2-6B was compared directly, the strains had generation times of 132 and 84 min, respectively (data not shown). As discussed below, *SHP1* was analyzed (as open reading frame YBL0515) in the course of sequencing chromosome II (43); in that analysis, a mutant strain bearing an *shp1* disruption allele had a generation time in liquid YPD of 145 min, compared with 90 min for an isogenic wild-type strain. This demonstrates that the growth defect of *shp1* mutants is intrinsic and unrelated to the *GAL10-GLC7* fusions present in the strains we have tested. Since *shp1-1* drastically reduces PP1 activity (see below), slow growth could be a result of transient arrest at the point or points in

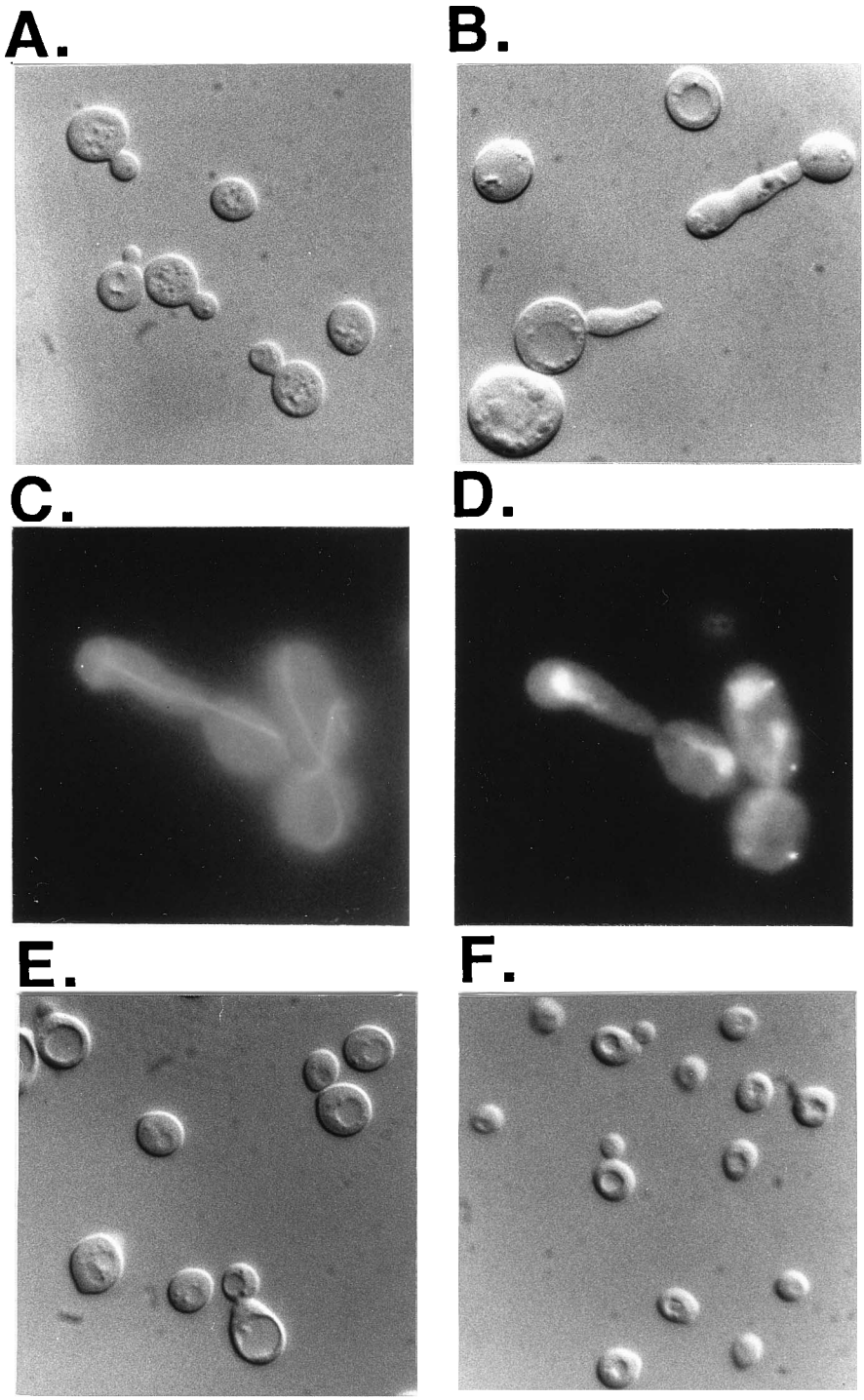

FIG. 5. Suppression of morphological consequences of *GLC7* overexpression by *shp1-1*. (A and B) Strain FVY92192 (*GAL10-GLC7 SHP1*) 12 h after inoculation from YPRaf into YPD (A) and YPGal (B). Nomarski differential interference contrast photomicrography. (C and D) *GAL10-GLC7*-arrested cells of strain FVY92206 (*GAL10-GLC7*/*GAL10-GLC7 SHP1*/*SHP1*) stained with anti-α-tubulin monoclonal antibody (C) and DAPI (D). (E and F) Strain FVY92215-9A (*GAL10-GLC7 shp1-1*) 12 h after inoculation into YPD (E) and YPGal (F). Nomarski differential interference contrast photomicrography. Magnification, ×100 (all panels).

G_2/M when Glc7p activity is required for cell cycle progression (23; also see below). However, although we have not rigorously ruled out this explanation, in none of the *shp1* mutant strains which we have examined have we observed the major elevation in the percentage of large-budded cells that such a mechanism would predict (Fig. 5 and data not shown).

The *shp1-1* mutation reduces cellular PP1 activity without affecting either the steady-state level of Glc7p or its subcellular localization, which is mainly nuclear. To account for the suppression of *GLC7* overexpression lethality by *shp1-1* and for the Glc^- and Spo^- secondary phenotypes associated with this mutation, we investigated the effects of the *shp1-1* muta-

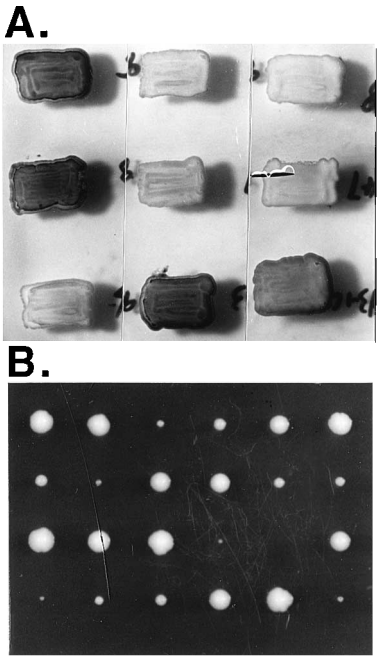

FIG. 6. Glc$^-$ and slow-growth phenotypes of *shp1* mutants. (A) Patches of cells grown on a YPD plate were stained with I_2-KI solution to reveal the glycogen content. Top, left to right: FVY91175 (*shp1-1*/*SHP1*), FVY92008 (*shp1-2*/*shp1-2*), FVY91131 (*shp1-1*); middle, left to right: FVY91193 (*shp1-2*/*SHP1*), FVY92007 (*shp1-1*/*shp1-1*), FVY9147 (*shp1-2*); bottom, left to right: FVY92006 (*shp1-1*/*shp1-2*), FVY91123 (*SHP1*/*SHP1*), RCY3-1C (*SHP1*). (B) Tetrad dissection of meiotic spores of strain FVY93142 (*SHP1*/*shp1-1*) on YPD.

tion on cellular PP1 activity and on the steady-state level and intracellular location of Glc7p. Figure 7A and B shows the level of dephosphorylation activity directed against glycogen phosphorylase *a* in *SHP1*$^+$ and *shp1-1* cells. In the experiment shown in Fig. 7A, extracts of wild-type (left graph) and *shp1-1* (right graph) cells were analyzed by DEAE-cellulose chromatography. In both strains, the only functional *GLC7* gene was a fusion (described below) of the coding region to an influenza virus HA epitope-encoding sequence, carried on a centromeric plasmid. Column fractions were assayed for PP activity in the presence (solid line) and absence (dotted line) of 2 nM okadaic acid (a concentration chosen to selectively inactivate PP2A) and for the presence of Glc7p by Western blotting with anti-HA monoclonal antibody. Figure 7B shows the results of a separate experiment in which Glc7p was expressed from the normal *GLC7* locus alone (solid lines) or from the *GLC7* locus and an induced *GAL10-GLC7* fusion locus (dotted lines) in an

TABLE 3. Sporulation of suppressive and nonsuppressive diploid strains

Strain	Relevant genotype	% Sporulation[a]
FVY91123	*SHP1*/*SHP1*	8.0
FVY91175	*shp1-1*/*SHP1*	8.7
FVY91193	*shp1-2*/*SHP1*	7.9
FVY92007	*shp1-1*/*shp1-1*	0
FVY92008	*shp1-2*/*shp1-2*	0
FVY92006	*shp1-1*/*shp1-2*	0

[a] Sporulation was induced on plates (40), and the cultures were inspected microscopically for spore formation. A total of 1,000 cells of each culture were scored.

TABLE 4. Tetrad analysis of strain FVY93142[a]

Parental phenotype[b]	Frequency of tetrad type[c]		
	PD	T	NPD
Shp$^+$ Glc$^+$ × Shp$^-$ Glc$^-$	25	0	0
Shp$^+$ Spo$^+$ × Shp$^-$ Spo$^-$	25	0	0
Shp$^+$ Large × Shp$^-$ Small	26	0	0
Shp$^+$ His$^-$ × Shp$^-$ His$^+$	3	20	3

[a] Relevant genotype, *SHP1*/*shp1-1 his3*Δ/*HIS3*::*GAL10-FLP1 lys2*::(*LEU2 GAL10-GLC7*)/*lys2*::(*LEU2 GAL10-GLC7*).

[b] Large and Small refer to the sizes of spore colonies after 2 or 3 days. Shp phenotypes were scored by replica plating to YPGal to induce transcription of the *GAL10-GLC7* fusion. Glc phenotypes were scored by iodine staining. Spo phenotypes were scored by mating segregants with *shp1-1* haploid tester strains, inducing sporulation of the resulting diploid strains on plates (40), and inspecting the cultures microscopically for spore formation. Diploid derivatives of Spo$^+$ isolates formed tetrads at a frequency of 10^{-2} to 10^{-1} cells, and those of Spo$^-$ isolates never formed visible spores ($<10^{-4}$ cells).

[c] PD, parental ditype; T, tetratype; NPD, nonparental ditype.

SHP$^+$ strain (left graph) or an *shp1-1* strain (right graph). In this experiment, all PP assay mixtures included 2 nM okadaic acid.

In the first experiment, the resistance of the first peak to inhibition by 2 nM okadaic acid identifies it as PP1; recovery of the Glc7-HA fusion polypeptide in first-peak fractions is consistent with this assignment. In the second experiment, the increase in PP activity upon galactose induction confirms that the single remaining, okadaic acid-resistant peak was due to Glc7p. In both experiments, it is apparent that the *shp1-1* mutation strongly depressed PP1 activity; furthermore, its relative effect was greater in the cells overproducing Glc7p from the *GAL10-GLC7* fusion, which would be consistent with its product being limiting for PP1 activity. The variation between the basal (uninduced) levels of PP1 activity in wild-type cells in the two experiments may have been caused by the different levels of protein loaded on the columns, the use of wild-type versus HA-tagged Glc7p, location of the active copy of *GLC7* or *GLC7*::HA on a chromosome versus a centromeric plasmid, different batches of labeled substrate, or some combination of these factors (see figure legends and Materials and Methods for detailed experimental conditions). In any event, it does not vitiate the conclusion that *shp1-1* decreases Glc7p-PP1 activity, since that conclusion rests entirely on comparisons within the individual experiments.

To determine whether the effect of the *shp1-1* mutation on cellular PP1 activity was mediated by a decrease in Glc7p polypeptide level, we introduced a fusion of *GLC7* and a sequence encoding an influenza virus HA epitope, carried on centromeric plasmid CB597 (49), into isogenic *shp1-1* and *SHP1*$^+$ strains and detected the fusion polypeptide by Western blotting using an anti-HA monoclonal antibody. To ensure the biological relevance of the Glc7p-HA fusion protein, in the strain used for this experiment the chromosomal *GLC7* locus contained the lethal *glc7*::*LEU2* allele described above, so that the only source of the essential function of Glc7p was the fusion gene. These cells grew normally, and, as expected, viable cells lacking the plasmid *URA3* marker could not be isolated after growth in YPD; additionally, these cells were Glc$^-$, while the *SHP1*$^+$ *glc7*::*LEU2* [*GLC7*::HA] strain FVY903044 was Glc$^+$, indicating that the Glc7p-HA fusion responded to the genotype of the *SHP1* locus in the same way as wild type Glc7p (data not shown). The Western blot results (Fig. 7C) did not show a difference between the polypeptide levels in the *shp1-1* and *SHP1* strains that could account for the previously observed difference in PP1 activity.

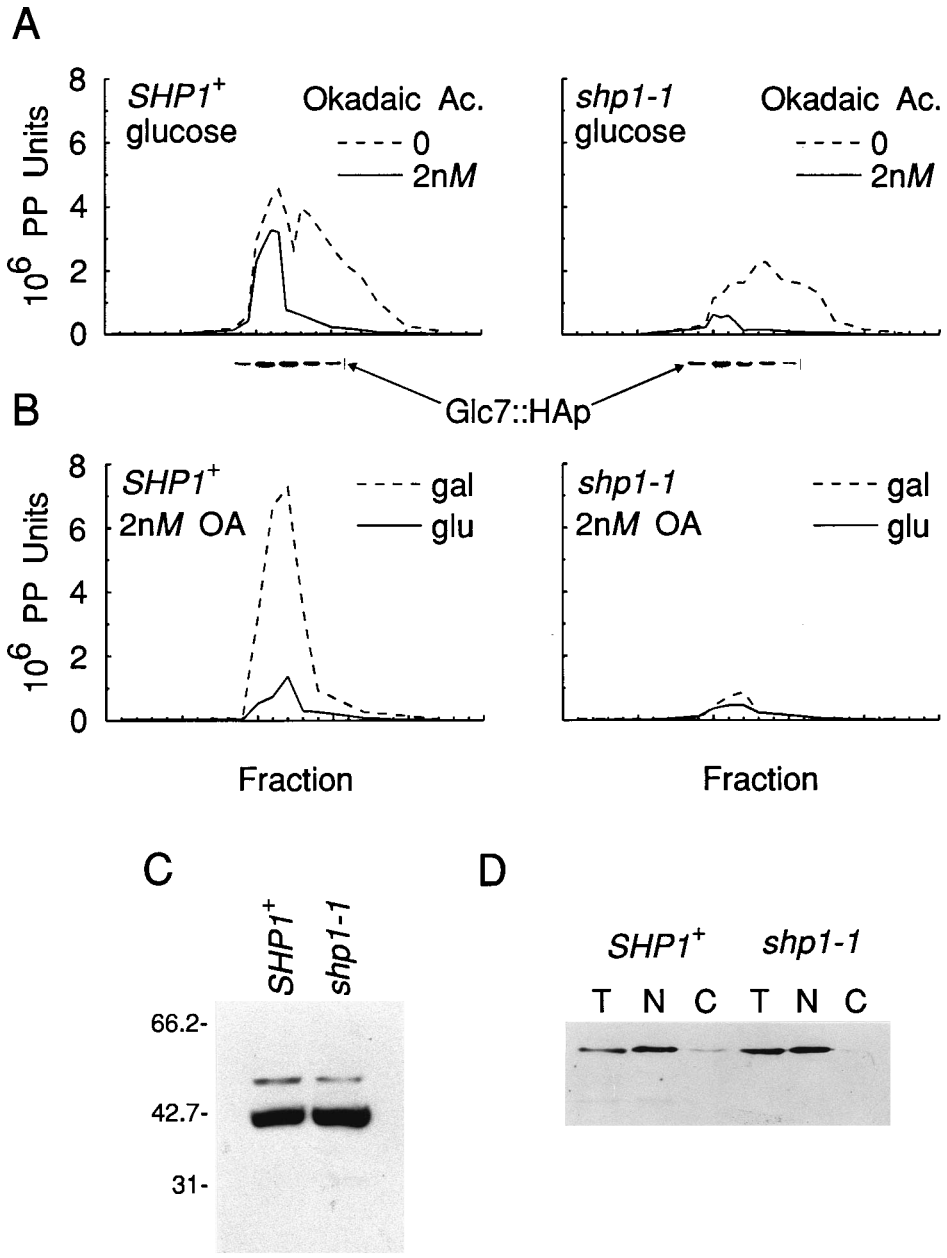

FIG. 7. Effect of *shp1-1* on PP1 activity and on the steady-state level and nuclear localization of Glc7-HA protein. (A) DEAE-cellulose chromatography of extracts of strain FVY93044 (*SHP1 glc7*::*LEU2* [*GLC7*::HA]) (left graph) and strain FVY93149 (*shp1-1 glc7*::*LEU2* [*GLC7*::HA]) (right graph) cells. Columns were loaded with 4 μg of total cellular protein. Dashed lines represent total PP activity, and solid lines represent activity in the presence of 2 nM okadaic acid. Computer scans of Western blots of fractions 18, 21, 24, 27, and 30, developed with anti-HA monoclonal antibody, are shown below the *x* axis; no fractions before or after these contained detectable Glc7-HA protein. (B) DEAE-cellulose chromatography of extracts of strain FVY92192 (*SHP1 GLC7 GAL10-GLC7*) (left graph) and strain FVY92215-9A (*shp1-1 GLC7 GAL10-GLC7*) (right graph), made from cells growing in YPD (solid lines) and from cells incubated for 2 h in YPGal after inoculation from YPRaf (dashed lines). Columns were loaded with 3 μg of total cellular protein, and all assays included 2 nM okadaic acid, which was shown to inhibit PP2A activity in the previous experiment. (C) Western blot of crude lysates of YPD cultures of strains FVY93044 (*SHP1 glc7*::*LEU2* [*GLC7*::HA]; labeled *SHP*) and FVY93043 (*shp1-1 glc7*::*LEU2* [*GLC7*::HA]; labeled *shp*) cells, developed with anti-HA monoclonal antibody. Each lane was loaded with 10 μg of protein. (D) Western blot of total (T), nuclear (N), and cytoplasmic (C) proteins of the same strains as in panel C with the same antibody. The T and C lanes were loaded with 10 μg of protein, and the N lanes were loaded with 5 μg. For both Western blots, equal loading and lack of gross protein degradation were confirmed by Coomassie brilliant blue-stained gels run in parallel (data not shown).

Because in some cases the biological functions of PP1 may be regulated by modulation of its intracellular location (14, 19, 44), we investigated the effects of *shp1-1* on the localization of the Glc7p-HA fusion polypeptide. Immunofluorescent staining indicated a predominantly but not exclusively nuclear location (data not shown), which is consistent with the results observed for *dis2*$^+$-PP1 in *S. pombe* (32). We therefore compared the partitioning of the polypeptide between nuclear and cytoplasmic fractions in wild-type and *shp1* cells by Western blotting. These results confirmed the predominantly nuclear localization but failed to demonstrate any difference between the two strains (Fig. 7D). We conclude from these and the previous

results that the *shp1* mutations were more likely to affect the catalytic activity of Glc7p than its production, localization, or turnover.

Depletion of Glc7p in an *shp1* strain results in arrest of the cell division cycle during mitosis. The suppression of the lethality of the induced *GAL10-GLC7* fusion by the *shp1* mutations permitted us to use *GAL10* promoter control to assess the phenotypic effects of loss of Glc7p function. We induced sporulation of the *glc7*::*LEU2*/*GLC7* [*URA3 GLC7*] heterozygote FVY93012(pJL5) and recovered three *shp1-1 lys2*::*GAL10-GLC7 glc7*::*LEU2* haploid segregants, all of which contained pJL5. After overnight growth of these strains in YPD, YPRaf, and YPGal liquid media, we streaked the cells onto plate media of the same composition and assessed the loss of the plasmid by replica plating to -Ura galactose medium. We observed plasmid loss in approximately 1% of cells that had been grown in YPGal but no plasmid loss in the other cultures (data not shown), leading us to conclude that the *GAL10-GLC7* fusion failed to supply the essential function of Glc7p during growth in glucose- or raffinose-based medium.

We then grew two of the plasmid-free descendants in YPGal liquid medium to midexponential phase (2×10^7 cells per ml), transferred the cells to YPD medium, and monitored the cultures at intervals for cell concentration and the percentage of viable and of budded cells. As expected, the return to growth on glucose resulted in gradual cessation of growth and loss of cell viability as the existing Glc7p was either turned over or diluted thorough cell division; as growth ceased, the percentage of budded cells in the cultures increased dramatically (Fig. 8 shows these results for one of the cultures). Microscopic examination revealed a preponderance of large-budded cells in the arrested population, consistent with stage-specific arrest at G_2/M. Staining of chromatin with DAPI and of microtubules with anti-α-tubulin monoclonal antibody showed 80% of nuclei in the large-budded cells to be bilobed and extending through the bud neck, with extended spindle fibers, a morphology consistent with late mitotic arrest. The remainder contained globular nuclei with short spindles, located near the bud neck in the mother cell, a morphology more consistent with G_2 or early mitotic arrest (Fig. 8). We conclude that the activity of Glc7p is required for entry into or completion of mitosis. This result resembles but differs in detail from early M-phase arrest caused by a *glc7*^{cs} mutation (23); possible explanations for the difference will be discussed below.

The *shp1* mutations are lesions in a gene of previously unknown biochemical function found on chromosome II. To identify the *SHP1* gene, we transformed the *shp1-1 GAL10-GLC7* strain FVY92189 with plasmid DNA from a YCp50-based yeast genomic library (39; plasmid-bearing bacterial cultures kindly provided by W. Chirico). We tested transformants for plasmid-dependent restoration of the overexpression lethality of *GAL10-GLC7*, specifically, the inability to grow on -Ura galactose plates, accompanied by the ability to grow normally on both -Ura glucose and YPGal plates. Among 20,000 primary yeast transformants, we identified 3 confirmed isolates, bearing clones from different library pools, which conferred this phenotype. We recovered the library clones in *E. coli*, determined by restriction mapping and stringent Southern hybridization that they contained overlapping genomic insertions (data not shown), and reintroduced them into mutant yeast cells, where they all complemented both *shp1-1* and *shp1-2* (Fig. 9). We also tested the ability of cloned copies of the wild-type alleles of *GLC1*, *GLC4*, and *GLC8*, which were carried on plasmids pd13, pd46, and p1833 and which encode the two isoforms of Ras2p GTPase activator protein and a homolog of the mammalian heat-stable PP1 inhibitor-2, respectively (11), to complement *shp1-1* and *shp1-2*; they did not (data not shown).

By deletion and linker insertion mutagenesis of one of the library clones (primary complementing isolate 5), the sequences specific for its ability to restore the lethal phenotype were localized to the region immediately surrounding a *Bam*HI site (Fig. 9). We obtained 150 bases of DNA sequence adjacent to this site which exactly matched the sequence of an open reading frame designated YBL0515, which had been identified during a chromosome II sequencing project and whose disruption had resulted in asporogenesis and slow growth (43). The sequence of *SHP1* predicts a 432-amino-acid protein with a molecular mass of 47 kDa and a pI of 4.63. Its predicted amino acid sequence is not strongly homologous to any other sequence on deposit in the public databases (BLASTP and TBLASTN searches of the nonredundant union set of sequences on deposit at the National Library of Medicine [1]), and a search for protein functional consensus sequences was uninformative except for identification of a number of potential sites for posttranslational modification, most notably one site for phosphorylation by cAMP-dependent protein kinase and eight each for phosphorylation by protein kinase C and casein kinase II (IntelliGenetics PC/GENE PROSITE search [5]).

To confirm that the complementing clones contained *SHP1*, we subcloned part of the genomic insert found in isolate 5 into the *URA3*-marked integrating vector YIp5; used a *Pme*I digest of the resulting plasmid, pSRZ27, for targeted integrative transformation of the *SHP1*$^+$ *GAL10-GLC7* strain FVY92192; and obtained chromosomal integrants carrying the plasmid at the locus homologous to the library insert. In a cross of one such integrant with the *shp1-1 GAL10-GLC7* strain FVY92215-2D, 29 of 29 meiotic tetrads exhibited a parental ditype segregation pattern of Ura$^+$ Shp$^+$ and Ura$^-$ Shp$^-$, indicating that the cloned locus was tightly linked to *SHP1*. This and the similarity of the secondary phenotypes of the *shp1* mutants to those resulting from interruption of YBL0515 (43) lead us to conclude that they are the same gene.

DISCUSSION

The broad substrate specificity of PP1 naturally raises the question of how modulation of its activity can be exploited in the control circuits that govern individual biological processes. An answer to this question which has received much experimental validation is that the PP1 catalytic subunit ($PP1_c$) forms complexes with regulatory subunits which target it to particular subcellular compartments, thus endowing the holoenzyme with more in vivo specificity than is apparent in vitro (reviewed in references 14 and 44). The clearest example of this is the G (glycogen-binding) subunit, encoded in *S. cerevisiae* by *GAC1* (19, 45), whose physical association with $PP1_c$ is specifically required for the stimulation of glycogen biosynthesis by PP1.

The phenotypic and biochemical effects of *shp1* mutant alleles, presented here, suggest another mechanism for the differential regulation of PP1-dependent processes: modulation of Glc7p catalytic activity in an environment in which different processes have different requirements for such activity. Our EMS-induced *shp1* mutations markedly reduce Glc7p catalytic activity without noticeably affecting the level or distribution of the protein. They produce strong phenotypes referable to the involvement of Glc7p in a subset of its dependent pathways—sporulation (absolute defect), glycogen biosynthesis, and whatever process(es) is lethally deranged by overproduction of the wild-type protein—without abolishing or seriously perturbing the essential G_2/M function. Further reduction of Glc7p activ-

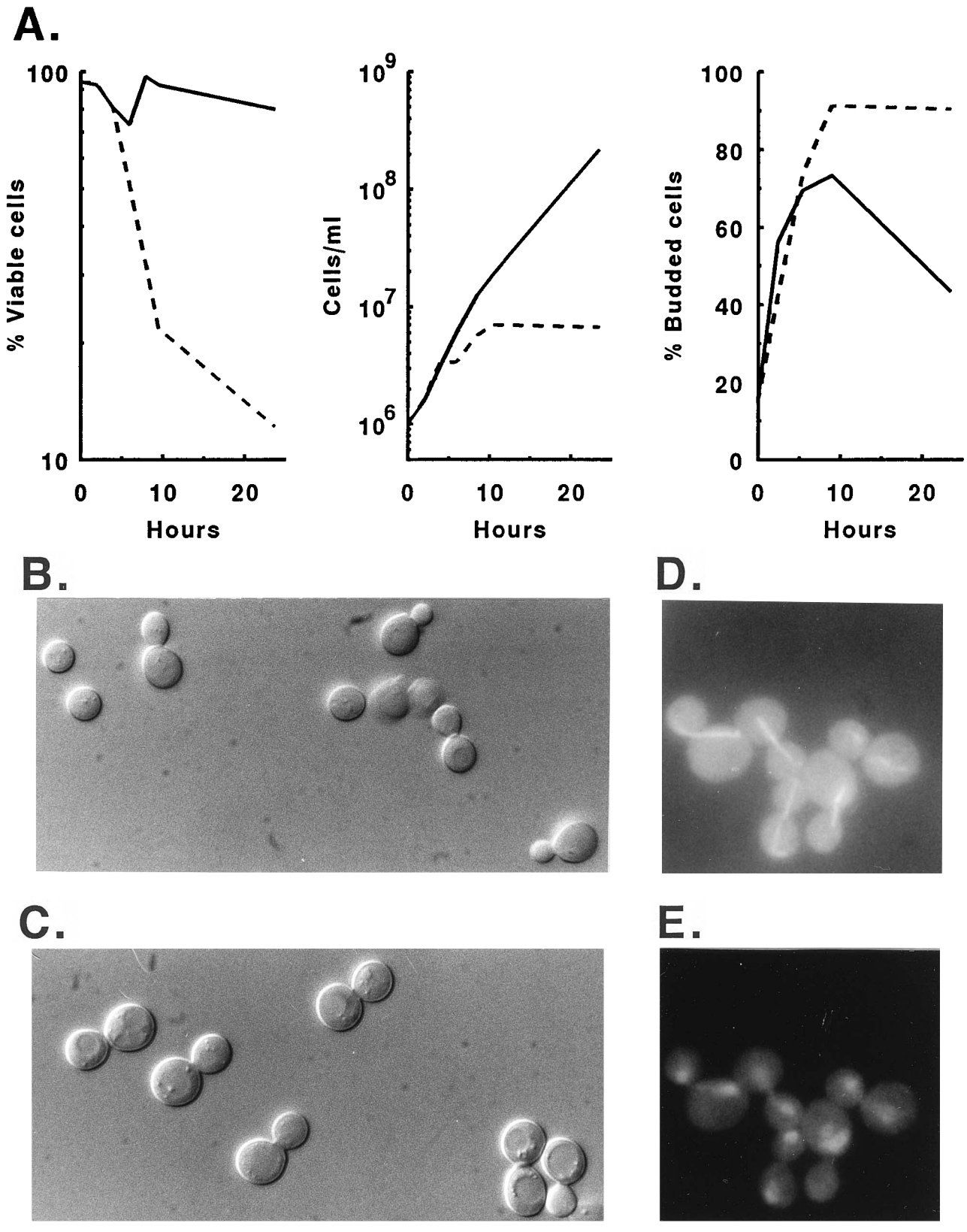

FIG. 8. Effect of depletion of Glc7p from *shp1-1* cells. (A) Kinetics of death (left), growth arrest (middle), and accumulation of budded cells (right) in a culture of strain FVY93014 (*glc7*::*LEU2 GAL10-GLC7 shp1-1*) after transfer from YPGal to YPD medium. Solid line, YPGal; dotted line, YPD. (B and C) Morphology of FVY93014 cells during exponential growth in YPGal (B) and 8 h after inoculation into YPD (C). Nomarski differential interference contrast photomicrography. (D and E) Glucose-arrested FVY93014 cells stained with anti-α-tubulin antibody (D) and DAPI (E). Magnification, ×100 (panels B through E).

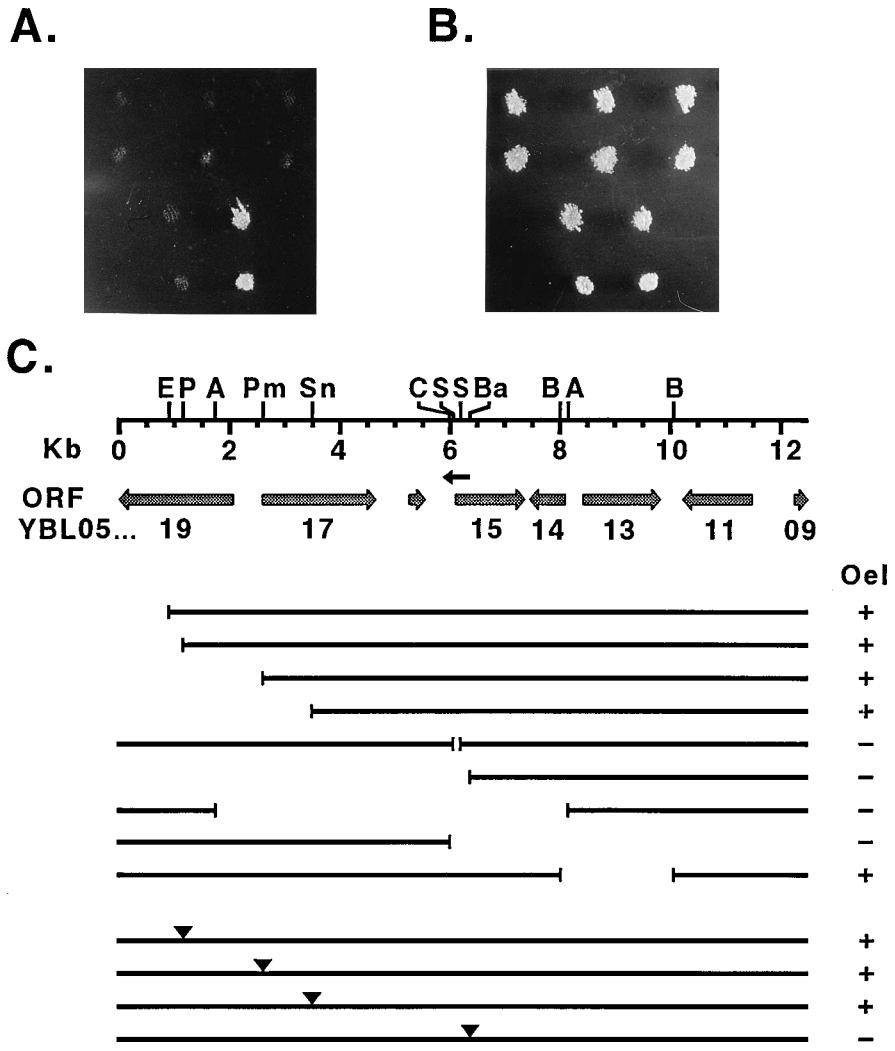

FIG. 9. Complementation of *shp1-1* and *shp1-2* by YBL0515. (A and B) Transformants of *shp1* mutant and control strains were replica plated from −Ura glucose medium to −Ura galactose (A) and −Ura glucose (B). Top row (left to right): FVY92189 (*GAL10-GLC7 shp1-1*) bearing primary complementing YCp50 library isolates 5, 16, and 30. Second row (left to right): FVY93140 (*GAL10-GLC7 shp1-2*) bearing the same plasmids. Third row (left to right): FVY92186 (*GAL10-GLC7 SHP1*) bearing pJH5 and FVY92189(YCp50). Bottom row (left to right): FVY92186(pJH5) and FVY93140(YCp50). (C) Mutational analysis of isolate 5. The restriction map shown is that predicted by the sequence of the region (43); our empirical map of the insert agrees on the order and approximate spacing of all of the sites shown, except that we failed to detect one of the two closely spaced *Swa*I sites (data not shown). The numbered open reading frames are those described in reference 43; YBL0509 and YBL0519 are predicted to be 3′ truncated in this isolate. The small black arrow represents the sequence we determined. Deletion mutations are shown as gaps, and frameshifting *Not*I linker insertions are shown as triangles. Restoration of the overexpression lethal phenotype of the *GAL10-GLC7* fusion in the *shp1-1* strain FVY92189 by the mutants was scored as described for panel A (data not shown). Abbreviations: ORF, open reading frame; Oel, overexpression lethality of the *GAL10-GLC7* fusion; A, *Afl*II; B, *Bst*EII; Ba, *Bam*HI; C, *Cla*I; E, *Eag*I; P, *Pvu*II, Pm, *Pme*I; S, *Swa*I; Sn, *Sna*BI.

ity by shutoff of *GAL10-GLC7* in an *shp1* strain results in a lethal phenotype similar to that produced by $glc7^{cs}$ at its restrictive temperature (23). Ablation of *SHP1* is not lethal but, instead, has the same effects on growth and sporulation which we have observed for EMS-induced mutations (43). We conclude from these observations that Shp1p is a direct or indirect positive regulator of Glc7p activity; that the Shp1p-dependent, maximal activity of Glc7p is required for normal sporulation and glycogen accumulation and for overexpression lethality; and that a Shp1p-independent, basal level of Glc7p activity is sufficient for its essential G_2/M function(s). Thus, since widely variable levels of Glc7p activity are compatible with viability, there is latitude for physiological control of its other functions via control of Glc7p protein level or activity. This would not be incompatible with other, more specific controls, such as glycogen targeting by Gac1p; rather, it would be superimposed on them. The previous observation of an increase in the *GLC7* transcript level during the onset of stationary phase (17) is compatible with control at the level of gene expression, and regulation by Shp1p could provide posttranslational control.

How Shp1p regulates Glc7p is an open question. Although Shp1p could be a positive regulatory subunit like Gac1p, the observation that no polypeptide agreeing closely with the predicted native molecular weight of Shp1p is coimmunoprecipitated with Glc7-HAp (49) argues that its effects may be more indirect. By analogy with mamalian cells, in which $PP1_c$ is also regulated by physical association with inhibitory subunits (14, 44), one possible mode of indirect action of Shp1p would be the inactivation of such subunits. Also favoring an indirect role for Shp1p is the possibility that *shp1* mutations have pleiotropic effects on other PPs. In the experiment shown in Fig. 7A, it appears that there may be a negative effect of the mutant on

PP2A activity, although the absence of data on the level of PP2A protein and its recovery from the column and the lack of corroborating phenotypic data preclude a firm conclusion to that effect. The existence of a PP2A overproduction phenotype (35) could provide a test of this hypothesis.

In addition to what they tell us about *SHP1* itself, the data we have presented provide new information on the essential function(s) of PP1 in G_2/M progression and, to a lesser extent, on the mechanism of *GLC7* overexpression lethality. As was true for conditional alleles of its *Schizosaccharomyces* and *Aspergillus* homologs $dis2^+$ and *bimG*, a *cs* allele of *GLC7*, $glc7^{Y\text{-}170}$, conferred a cell cycle progression defect specific for this phase (15, 23, 31). However, although all three conditional alleles were recessive to wild type, $dis2\text{-}11^{cs}$ was clearly not a simple conditional-null mutant, since deletion of $dis2^+$ was not lethal (25, 32). Because of this and because a recessive lethal $glc7^{ts}$ allele did not confer stage-specific arrest (28), the possibility remained that the arrest conferred by $glc7^{Y\text{-}170}$ was an allele-specific effect and did not demonstrate a requirement for Glc7p catalytic activity per se at G_2/M (alternative models are discussed in reference 23). However, our depletion results unambiguously establish that such a requirement exists. Additionally, the difference in the predominant end points obtained with the $glc7^{cs}$ allele and with depletion (all early M versus 80% late M, respectively) is intriguing and merits further investigation. While it could represent an allele-specific or temperature-specific artifact of *cs* arrest or a natural difference in the responses of the strains to PP1 deficiency like the variation in response to Sit4p-PP deficiency among strains carrying different alleles at the polymorphic *SSD1* locus (48), it could also signal the existence of two closely temporally spaced PP1-dependent stage transitions, the latter of which might be hard to reveal by rapidly shutting off activity of the *cs* protein in unsynchronized cells. Discriminating among these possibilities will require exchanging the genetic backgrounds used in the depletion and *cs* arrest experiments, performing depletion experiments at the restrictive temperature of the *cs* mutation, and performing *cs* arrest experiments with synchronized cells.

With respect to the mechanism underlying *GLC7* overexpression lethality, the rapidity of arrest and viability loss which we observed (Fig. 4) argue against lethality being secondary to chromosomal nondisjunction events which occur in a low proportion of cells at lower levels of overexpression (18). As with extreme overproduction of PP2A (35), the morphological consequences of Glc7p overproduction which we observed are compatible with perturbation of the cell polarity/bud emergence machinery, with which *GLC7* has known genetic interactions (23). However, conclusions about the normal biological role of Glc7p must be drawn from overproduction data with great care, since the condition is unnatural and could have effects attributable to spillover of Glc7p activity into pathways normally regulated by other PPs. In the future, recovery of *shp* mutations acting downstream of Glc7p may shed light on this issue.

Finally, identification of control of Glc7p activity by Shp1p provides the first demonstration of the utility of the Hcl phenotype in pathway analysis and guidance for its future exploitation. Since the *shp1* mutations suppressed *GAL10-GLC7* lethality as well as the *GLC7* Hcl phenotype, they could have been recovered as suppressors of either lethal condition. Although there are cases in which an overexpression lethal gene does not exhibit lethality under both of these conditions, when it does, incorporation of both overexpression strategies into one suppressor screening strain could prevent recovery of the most common classes of false-positive isolates characteristic of each of them. These false-positive pseudo-suppressor classes—*trans* mutations affecting *GAL* promoter strength (16) and spontaneous diploid cells (our results)—appear to be specific for promoter-driven and template-driven overexpression, respectively; therefore, at least for some overexpression lethal genes, high-copy lethality and promoter-driven lethality could provide orthogonal approaches to suppressor mutation isolation, which, used in tandem, would be more powerful than either alone.

ACKNOWLEDGMENTS

We thank Kim Arndt, James Broach, John Cannon, William Chirico, and Mark Rose for generous gifts of strains, plasmids, and libraries; Maureen McLeod, Pamela Silver, and Ann Sutton for helpful discussions during the course of the work; Elizabeth Sylander for technical help; and our reviewers for their constructive suggestions. pJH5 was constructed by F.C.V. and J. Huo in the laboratory of James Broach, and we thank him for its use. pRC21 and RCY3-1C were constructed by Rouling Chang, and pJL5 was constructed by Jing Liu, both in our laboratory.

This research was supported by grants from the March of Dimes (Basil O'Connor Starter Scholar Award 5-758) and the National Institutes of Health (R01-GM-40614) to F.C.V. F.C.V. is an Established Investigator of the American Heart Association (grant 900248).

REFERENCES

1. **Altschul, S. F., W. Gish, W. Miller, E. W. Myers, and D. J. Lipman.** 1990. Basic local alignment search tool. J. Mol. Biol. **215:**403–410.
2. **Amati, B. B., and S. M. Gasser.** 1988. Chromosomal ARS and CEN elements bind specifically to the yeast nuclear scaffold. Cell **55:**976–978.
3. **Andreadis, A., Y.-P. Hsu, M. Hermodson, G. Kohlhaw, and P. Schimmel.** 1984. Yeast *LEU2*. J. Biol. Chem. **259:**8059–8062.
4. **Andreadis, A., Y.-P. Hsu, G. B. Kohlhaw, and P. Schimmel.** 1982. Nucleotide sequence of yeast *LEU2* shows 5′-noncoding region has sequences cognate to leucine. Cell **31:**319–325.
5. **Bairoch, A.** 1991. PROSITE: a dictionary of sites and patterns in proteins. Nucleic Acids Res. **19**(Suppl.)**:**2241–2245.
6. **Botstein, D., S. C. Falco, S. Stewart, M. Brennan, S. Scherer, D. T. Stinchcomb, K. Struhl, and R. Davis.** 1979. Sterile host yeast (SHY): a eukaryotic system of biological containment for recombinant DNA experiments. Gene **8:**17–24.
7. **Broach, J. R., V. R. Guarascio, and M. Jayaram.** 1982. Recombination within the yeast plasmid 2μ circle is site-specific. Cell **29:**227–234.
8. **Broach, J. R., and J. B. Hicks.** 1980. Replication and recombination functions associated with the yeast plasmid, 2μ circle. Cell **21:**501–508.
9. **Broach, J. R., J. N. Strathern, and J. B. Hicks.** 1979. Transformation in yeast: development of a hybrid cloning vector and isolation of the *CAN1* gene. Gene **8:**121–133.
10. **Broach, J. R., and F. C. Volkert.** 1991. Circular DNA plasmids of yeasts, p. 297–332. *In* J. R. Broach, J. R. Pringle, and E. W. Jones (ed.), The molecular biology of the yeast *Saccharomyces*: genome dynamics, protein synthesis, and energetics. Cold Spring Harbor Laboratory Press, Cold Spring Harbor, N.Y.
11. **Cannon, J. F., J. R. Pringle, A. Fiechter, and M. Khalil.** 1994. Characterization of glycogen-deficient *glc* mutants of *Saccharomyces cerevisiae*. Genetics **136:**485–503.
12. **Church, G. M., and W. Gilbert.** 1984. Genomic sequencing. Proc. Natl. Acad. Sci. USA **81:**1991–1995.
13. **Clarke, L., and J. Carbon.** 1980. Isolation of a yeast centromere and construction of functional small circular chromosomes. Nature (London) **287:** 504–509.
14. **Cohen, P.** 1989. The structure and regulation of protein phosphatases. Annu. Rev. Biochem. **58:**453–508.
15. **Doonan, J. H., and N. R. Morris.** 1989. The *bim*G gene of *Aspergillus nidulans*, required for completion of anaphase, encodes a homolog of mammalian phosphoprotein phosphatase 1. Cell **57:**987–996.
16. **Fedor-Chaiken, M., R. J. Deschenes, and J. R. Broach.** 1990. *SRV2*, a gene required for RAS activation of adenylate cyclase activity in yeast. Cell **61:** 329–340.
17. **Feng, Z., S. E. Wilson, Z.-Y. Peng, K. K. Schlender, E. M. Reimann, and R. J. Trumbly.** 1991. The yeast *GLC7* gene required for glycogen accumulation encodes a type 1 protein phosphatase. J. Biol. Chem. **266:**23796–23801.
18. **Francisco, L., W. Wang, and C. S. M. Chang.** 1994. Type 1 protein phosphatase acts in opposition to Ipl1 protein kinase in regulating yeast chromosome segregation. Mol. Cell. Biol. **14:**4731–4740.
19. **Francois, J. M., S. Thompson-Jaeger, J. Skroch, U. Zellenka, W. Spevak, and K. Tatchell.** 1992. *GAC1* may encode a regulatory subunit for protein phosphatase type 1 in *Saccharomyces cerevisiae*. EMBO J. **11:**87–96.
20. **Futcher, B., and J. Carbon.** 1986. Toxic effects of excess cloned centromeres.

Mol. Cell. Biol. **6:**2213–2222.
21. **Gibbs, J. B., and M. S. Marshall.** 1989. The *ras* oncogene—an important regulatory element in lower eukaryotic organisms. Microbiol. Rev. **53:**171–185.
21a. **Guha, S., and F. C. Volkert.** Unpublished observations.
22. **Hartley, J. L., and J. E. Donelson.** 1980. Nucleotide sequence of the yeast plasmid. Nature (London) **286:**860–864.
23. **Hisamoto, N., K. Sugimoto, and K. Matsumoto.** 1994. The Glc7 type 1 protein phosphatase of *Saccharomyces cerevisiae* is required for cell cycle progression in G_2/M. Mol. Cell. Biol. **14:**3158–3165.
24. **Ito, H., Y. Fukuda, K. Murata, and A. Kimura.** 1983. Transformation of intact yeast cells treated with alkali cations. J. Bacteriol. **153:**163–168.
25. **Kinoshita, N., H. Ohkura, and M. Yanagida.** 1990. Distinct, essential roles of type 1 and 2A protein phosphatases in the control of the fission yeast cell division cycle. Cell **63:**405–415.
26. **Liu, H., J. Krizek, and A. Bretscher.** 1992. Construction of a *GAL1*-regulated yeast cDNA expression library and its application to the identification of genes whose overexpression causes lethality in yeast. Genetics **132:**665–673.
26a. **Liu, J., and F. C. Volkert.** Unpublished data.
27. **Matsumoto, K., I. Uno, and T. Ishikawa.** 1985. Genetic analysis of the role of cAMP in yeast. Yeast **1:**15–24.
28. **Matsuura, A., and Y. Anraku.** 1994. Genetic interaction between the Ras-cAMP pathway and the Dis2s1/Glc7 protein phosphatase in *Saccharomyces cerevisiae*. Mol. Gen. Genet. **242:**257–262.
29. **McLeod, M., F. Volkert, and J. Broach.** 1984. Components of the site-specific recombination system encoded by the yeast plasmid 2-micron circle. Cold Spring Harbor Symp. Quant. Biol. **49:**779–787.
30. **Mortimer, R. K., C. R. Contopolou, and J. S. King.** 1992. Genetic and physical maps of *Saccharomyces cerevisiae*, edition 11. Yeast **8:**817–902.
31. **Ohkura, H., Y. Adachi, N. Kinoshita, O. Niwa, T. Toda, and M. Yanagida.** 1988. Cold-sensitive and caffeine-supersensitive mutants of the *Schizosaccharomyces pombe dis* genes implicated in sister chromatid separation during mitosis. EMBO J. **7:**1465–1473.
32. **Ohkura, H., N. Kinoshita, S. Miyatani, T. Toda, and M. Yanagida.** 1989. The fission yeast *dis2*$^+$ gene required for chromosome disjoining encodes one of two putative type 1 protein phosphatases. Cell **57:**997–1007.
33. **Peng, Z.-Y., R. J. Trumbly, and E. M. Reimann.** 1990. Purification and characterization of glycogen synthase from a glycogen-deficient strain of *Saccharomyces cerevisiae*. J. Biol. Chem. **265:**13871–13877.
34. **Pringle, J. R., A. E. M. Adams, D. G. Drubin, and B. K. Haarer.** 1991. Immunofluorescence methods for yeast. Methods Enzymol. **194:**565–602.
35. **Ronne, H., M. Carlberg, G.-Z. Hu, and J. O. Nehlin.** 1991. Protein phosphatase 2A in *Saccharomyces cerevisiae*: effects on cell growth and bud morphogenesis. Mol. Cell. Biol. **11:**4876–4884.
36. **Rose, M., P. Grisafi, and D. Botstein.** 1984. Structure and function of the yeast *URA3* gene: expression in *Escherichia coli*. Gene **29:**113–124.
37. **Rose, M. D., and J. R. Broach.** 1991. Cloning genes by complementation in yeast. Methods Enzymol. **194:**195–230.
38. **Rose, M. D., and G. R. Fink.** 1987. *KAR1*, a gene required for function of both intranuclear and extranuclear microtubules in yeast. Cell **48:**1047–1060.
39. **Rose, M. D., P. Novick, J. H. Thomas, D. Botstein, and G. R. Fink.** 1987. A *Saccharomyces cerevisiae* genomic plasmid bank based on centromere-containing shuttle vector. Gene **60:**237–243.
40. **Rose, M. D., F. Winston, and P. Hieter.** 1990. Methods in yeast genetics. Cold Spring Harbor Laboratory, Cold Spring Harbor, N.Y.
41. **Rothstein, R.** 1991. Targeting, disruption, replacement, and allele rescue: integrative DNA transformation in yeast. Methods Enzymol. **194:**281–301.
42. **Sambrook, J., E. F. Fritsch, and T. Maniatis.** 1989. Molecular cloning: a laboratory manual, 2nd ed. Cold Spring Harbor Laboratory Press, Cold Spring Harbor, N.Y.
43. **Scherens, B., M. El Bakkoury, F. Vierendeels, E. Dubois, and F. Messenguy.** 1993. Sequencing and functional analysis of a 32,560 bp segment on the left arm of yeast chromosome. II. Identification of 26 open reading frames, including the *KIP1* and *SEC17* genes. Yeast **9:**1355–1371.
44. **Shenolikar, S., and A. C. Nairn.** 1991. Protein phosphatases: recent progress. Adv. Second Messenger Phosphoprotein Res. **23:**1–121.
45. **Skroch Stuart, J., D. L. Frederick, C. M. Varner, and K. Tatchell.** 1994. The mutant type 1 protein phosphatase encoded by *glc7-1* from *Saccharomyces cerevisiae* fails to interact productively with the *GAC1*-encoded regulatory subunit. Mol. Cell. Biol. **14:**896–905.
46. **Stinchcomb, D. T., C. Mann, and R. W. Davis.** 1982. Centromeric DNA from *Saccharomyces cerevisiae*. J. Mol. Biol. **158:**157–179.
47. **Struhl, K., D. T. Stinchcomb, S. Scherer, and R. W. Davis.** 1979. High frequency transformation of yeast: autonomous replication of hybrid DNA molecules. Proc. Natl. Acad. Sci. USA **76:**1035–1039.
48. **Sutton, A., D. Immanuel, and K. T. Arndt.** 1991. The SIT4 protein phosphatase functions in late G_1 for progression into S phase. Mol. Cell. Biol. **11:**2133–2148.
49. **Sutton, A., F. Lin, M. J. F. Sarabia, and K. T. Arndt.** 1991. The *SIT4* protein phosphatase is required in late G_1 for progression into S phase. Cold Spring Harbor Symp. Quant. Biol. **56:**75–81.
50. **Tanaka, K., K. Matsumoto, and A. Toh-e.** 1989. *IRA1*, an inhibitory regulator of the *RAS*-cyclic AMP pathway in *Saccharomyces cerevisiae*. Mol. Cell. Biol. **9:**757–768.
51. **Tanaka, K., M. Nakafuku, T. Satoh, M. S. Marshall, J. B. Gibbs, K. Matsumoto, Y. Kaziro, and A. Toh-e.** 1990. S. cerevisiae genes *IRA1* and *IRA2* encode proteins that may be functionally equivalent to mammalian *ras* GTPase activating protein. Cell **60:**803–807.
52. **Toda, T., I. Uno, T. Ishikawa, S. Powers, T. Kataoka, D. Broek, S. Cameron, J. Broach, K. Matsumoto, and M. Wigler.** 1985. In yeast, *RAS* proteins are controlling elements of adenylate cyclase. Cell **40:**27–36.
53. **Vieira, J., and J. Messing.** 1982. The pUC plasmids, an M13mp7-derived system for insertion mutagenesis and sequencing with synthetic universal primers. Gene **19:**259–268.
53a. **Volkert, F. C.** Unpublished data.
54. **Volkert, F. C., and J. R. Broach.** 1986. Site-specific recombination promotes plasmid amplification in yeast. Cell **46:**541–550.
54a. **Volkert, F. C., J. Huo, and J. R. Broach.** Unpublished data.
55. **Wek, R. C., J. F. Cannon, T. E. Dever, and A. G. Hinnebusch.** 1992. Truncated protein phosphatase GLC7 restores translational activation of *GCN4* expression in yeast mutants defective for the eIF-2α kinase GCN2. Mol. Cell. Biol. **12:**5700–5710.
56. **Zhang, S.** Unpublished data.
57. **Zhang, S., and F. C. Volkert.** Unpublished data.